Numerical Analysis of Hydrogen Diffusion Problems Using the Finite Element Method

Hiroshi KANAYAMA*, Takanori SHINGOH**, Stephane NDONG-MEFANE**, Masao OGINO*, Ryuji SHIOYA* and Hiroshi KAWAI***

* *Department of Intelligent Machinery and Systems, Faculty of Engineering, Kyushu University and AIST, Fukuoka*
** *Department of Intelligent Machinery and Systems, Graduate School of Engineering, Kyushu University, Fukuoka*
*** *Keio University and AIST, Tokyo*

Abstract

This paper focuses on the Krom et al. hydrogen diffusion model in materials. Using the Sofronis and McMeeking model, we reconstruct our own finite element scheme based on the Krom et al. scheme, and apply the Galerkin method in this first trial. Results obtained with our new scheme are compared with previous results obtained by Sofronis and McMeeking, and Krom et al. to show good agreement.

List of symbols

Roman symbols:

$b_0[m]$: Crack tip opening (const).

$b[m]$: $4.7\,b_0$ (const).

$C_{L/T}[m^{-3}]$: Number of hydrogen atoms per unit volume in lattice/trap sites.

$C_b[m^{-3}]$: Boundary value of C_L (const).

$C_{L0}[m^{-3}]$: Initial hydrogen concentration (const).

$C_L^*[-]$: Test function for C_L.

$D_L[m^2 \cdot s^{-1}]$: Diffusion constant (const).

$D^*[-]$: $\dfrac{C_L + C_T(1-\theta_T)}{C_L}$.

$E[N \cdot m^{-2}]$: Young's modulus (const).

$f_i(\nu,\theta)[-]$: Universal function for plain strain.

$G[N \cdot m^{-2}]$: Shear modulus (const).

$h[m]$: Model thickness (const).

$J[s^{-1} \cdot m^{-2}]$: Hydrogen flux.

$K_I[MPa\sqrt{m}]$: Stress intensity factor (const).

$K_T[-]$: Trap equilibrium constant (const).

$M_L[m^2 \cdot s^{-1} \cdot mol \cdot J^{-1}]$: Mobility of the hydrogen in lattice sites (const).

$n[-]$: Outward normal vector or time step in the case of superscript.

$n'[-]$: Hardening exponent (const).

$N_{L/T}[m^{-3}]$: Number of lattice/trap sites per unit volume (N_L: const).

$R[J \cdot mol^{-1} \cdot K^{-1}]$: Gas constant (const).

$\mathbf{R}[m]$: Model radius (const).

$r[m]$: Radial component ($r = \sqrt{x^2 + y^2}$).

$T[K]$: Absolute temperature (const).

$\mathrm{T}[N.m^{-2}]$: Traction vector.

$t[s]$: Time.

$u_i[m]$: Displacement component.

$\overline{V}_H[m^3 \cdot mol^{-1}]$: Partial molar volume of hydrogen (const).

$x[m]$: Coordinate component x .

$y[m]$: Coordinate component y .

Greek symbols:

Γ_E : On Γ_E , the number of hydrogen atoms per unit volume is given.

Γ_N : On Γ_N , the flux through the surface is given.

$\partial\Omega = \Gamma$: Boundary of Ω .

$\Delta E_T[J \cdot mol^{-1}]$: Trap binding energy (const).

$\Delta t[s]$: Time interval (const).

$\varepsilon[-]$: Total strain.

$\varepsilon_P[-]$: Plastic strain.

$\theta_{L/T}[-]$: Ratio of the number of occupied sites to the total available for lattice/trap sites.

$\theta[rad]$: Angle.

$\mu_L[J \cdot mol^{-1}]$: Chemical potential in lattice sites.

$\mu_L^0[J \cdot mol^{-1}]$: Chemical potential in lattice sites at a reference temperature and pressure (const).

$\nu[-]$: Poisson ratio (const).

$\sigma[N \cdot m^{-2}]$: Applied stress.

$\sigma_h[N \cdot m^{-2}]$: Hydrostatic stress.

$\sigma_y[N \cdot m^{-2}]$: Yield stress (const).

$\sigma_{ij}[N \cdot m^{-2}]$: Stress tensor component.

Ω : Domain.

1. Introduction

In spite of decades of research effort, hydrogen assisted cracking is still the most serious problem in the world of hydrogen usage. Hydrogen embrittlement is still not clearly understood, and elastic-plastic stress analysis coupled with diffusion computation is needed to model the effects of hydrogen distribution in a solid. The finite element method (FEM) is a very useful tool for this purpose. P. Sofronis and R. M. McMeeking [1] proposed the FEM model to show the effects of hydrostatic stress and the trapping phenomenon for hydrogen distribution in plastically deformed steel. They investigated the hydrogen concentration near a blunting crack tip under small-scale yielding conditions, but unfortunately, their hydrogen transport model didn't provide the correct balance of hydrogen concentration into the considered material. Based on their work, another model providing the correct balance of hydrogen and showing a strong dependence of the hydrogen concentration in lattice sites on the strain rate was developed by Krom et al. [2].

This paper focuses on this new model. We reconstruct our own finite element scheme and apply the backward time difference with a suitable linearization as the pioneers. The resultant finite element scheme produces a non-symmetric coefficient matrix for each time step, though the original two papers deal with a symmetric matrix for each time step. Our approach is a standard one for the non-linear advection-diffusion equation. However, it has the conservative advection term which depends on absolute values of the hydrostatic stress gradient. So if these absolute values are larger, then the Péclet number becomes larger and some numerical oscillations will appear. One remedy is a well known stabilization technique. However the stabilization technique for the conservative advection term is not well known. So, the Galerkin method is applied in this first trial. In fact, some numerical difficulties are encountered for great absolute values of the hydrostatic stress gradient. This problem will be overcome by the use of the stabilization technique, for example. With a fully coupled analysis, they are our next goals for hydrogen diffusion problems in materials, and will be mentioned in the forthcoming papers.

2. The hydrogen transport equation

2.1 The original model

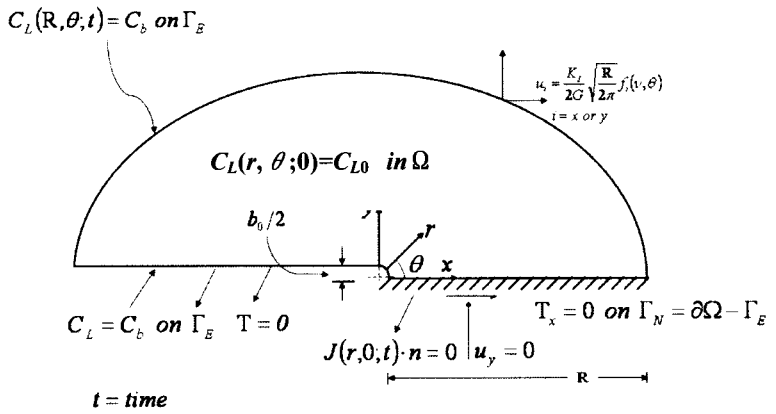

Fig 1. Description of the boundary and initial conditions for the one side coupled diffusion and elastic-plastic problem under small scale yielding conditions [1].

The original model is based on the Sofronis and McMeeking model [1], which is based on the equilibrium theory established by Oriani [3]. Hydrogen transport between trap sites is made by lattice diffusion [2]. Trap sites can be found at micro structural defects [1)4)], and are assumed not to form an extended network; they are supposed to be reversible and saturable [1)2)]. The main difference between the Sofronis and McMeeking model and the Krom et al. model [2] is a factor depending on the strain rate in order to get the correct balance of hydrogen concentration.

In **Fig 1**, we consider a body with the volume Ω and the surface $\partial\Omega = \Gamma$. Because of the mass conservation law, the rate of change of total hydrogen inside Ω is equivalent to the flux through Γ. Constants C_h and C_{L0} are given numbers of hydrogen atoms per unit volume in Normal Interstitial Lattice Sites (NILS). J is the hydrogen flux, u_i displacement components, and T the traction vector [1].

$$\frac{\partial}{\partial t}\int_{\Omega}\{C_L + C_T\}d\Omega + \int_{\partial\Omega} J\cdot n dS = 0,$$
$$J = -M_L C_L \nabla\mu_L \quad \& \quad \mu_L = \mu_L^0 + RT\log_e\frac{C_L}{N_L} - \overline{V}_H\sigma_h. \tag{1}$$

C_L and C_T are respectively the number of hydrogen atoms per unit volume in lattice sites and in trap sites. J is the hydrogen flux, n is the outward normal vector, M_L is the mobility of the hydrogen in the lattice sites, N_L is the number of lattice sites per unit volume, and μ_L is the chemical potential in lattice sites. R is the gas constant, T is the absolute temperature, μ_L^0 is the chemical potential at a reference temperature and pressure, and σ_h is defined as the hydrostatic stress, such that $\sigma_h = \frac{1}{3}\sum_{i=1}^{3}\sigma_{ii}$, where the component σ_{ij} is the stress tensor component. The subscripts i and j are usually denoted x, y, z instead of 1, 2 and 3. $\overline{V}_H$ is the partial molar volume of hydrogen.

Using the expression of μ_L, the hydrogen flux can be expressed with the lattice diffusivity D_L as

$$J = -D_L\nabla C_L + \frac{D_L C_L \overline{V}_H}{RT}\nabla\sigma_h, \tag{2}$$
$$D_L = M_L RT.$$

After substituting **(2)** in **(1)**, and applying the divergence theorem, we obtain for the arbitrary volume Ω

$$\frac{\partial C_L}{\partial t} + \frac{\partial C_T}{\partial t} - \nabla\cdot(D_L\nabla C_L) + \nabla\cdot\left(\frac{C_L D_L \overline{V}_H}{RT}\nabla\sigma_h\right) = 0. \tag{3}$$

The hydrogen concentrations are first related to the numbers of sites

$$C_L = \theta_L N_L, \tag{4}$$
$$C_T = \theta_T N_T, \tag{5}$$

where θ_L and θ_T are respectively the occupancy of lattice sites and the occupancy of trap sites, and N_L and N_T are the lattice site and the trap site densities. An expression of the hydrogen concentration in trap sites as a function of concentration in lattice sites given by Oriani [3] in the case of the equilibrium is, under the assumption that $\theta_L << 1$,

$$C_T = \frac{N_T}{1 + \dfrac{1}{K_T \theta_L}}, \tag{6}$$

where K_T is the equilibrium constant such that $K_T = e^{-\Delta E_T / RT}$ with ΔE_T as the trap binding energy. The partial derivative of the hydrogen concentration in trap sites with respect to time is

$$\frac{\partial C_T}{\partial t} = \frac{\partial C_T}{\partial C_L}\frac{\partial C_L}{\partial t} + \frac{\partial C_T}{\partial N_T}\frac{dN_T}{d\varepsilon_p}\frac{\partial \varepsilon_p}{\partial t}, \tag{7}$$

with ε_p as the plastic strain. The final equation presented by Krom et al. [2] for hydrogen transport is

$$\frac{C_L + C_T(1-\theta_T)}{C_L}\frac{\partial C_L}{\partial t} - \nabla\cdot\left(D_L \nabla C_L\right) + \nabla\cdot\left(\frac{C_L D_L \overline{V}_H}{RT}\nabla\sigma_h\right) + \theta_T \frac{dN_T}{d\varepsilon_p}\frac{\partial \varepsilon_p}{\partial t} = 0. \tag{8}$$

2.2 The weak form

The multiplication by a test function of (8) and integration over Ω produces

$$\int_\Omega C_L^* \left\{ D^* \frac{\partial C_L}{\partial t} - \nabla\cdot\left(D_L \nabla C_L\right) + \nabla\cdot\left(\frac{C_L D_L \overline{V}_H}{RT}\nabla\sigma_h\right) + \theta_T \frac{dN_T}{d\varepsilon_p}\frac{\partial \varepsilon_p}{\partial t} \right\} d\Omega = 0, \tag{9}$$

where C_L^* is the test function, and using the Green's theorem in **(9)**, the following result is obtained.

$$\int_\Omega \left\{ \begin{array}{l} C_L^* D^* \dfrac{\partial C_L}{\partial t} + \nabla C_L^* D_L \nabla C_L - \nabla C_L^* \cdot \dfrac{C_L D_L \overline{V}_H}{RT}\nabla\sigma_h \\ + C_L^* \theta_T \dfrac{dN_T}{d\varepsilon_p}\dfrac{\partial \varepsilon_p}{\partial t} \end{array} \right\} d\Omega + \int_{\partial\Omega} C_L^* J\cdot n\, dS = 0, \tag{10}$$

where

$$D^* = \frac{C_L + C_T(1-\theta_T)}{C_L}. \tag{11}$$

Considering the concentration fixed on the surface Γ_E, we have $C_L^* = 0$ on Γ_E. Also, we have $J \cdot n = 0$ on Γ_N. Therefore we have $\int_{\partial\Omega} C_L^* J \cdot n \, dS = 0$. A detailed expression of θ_T as a function of C_L is needed as follows.

Using **(4), (5)** and **(6)**, we can find

$$\theta_T = \frac{1}{1 + \dfrac{N_L}{K_T C_L}} = \frac{K_T C_L}{K_T C_L + N_L}. \tag{12}$$

Also, we have

$$C_T = \frac{N_T K_T}{K_T + N_L / C_L} = \frac{C_L N_T K_T}{K_T C_L + N_L}. \tag{13}$$

Then, after using **(12)** and **(13)**, D^* has the following expression

$$D^* = 1 + \left[\frac{N_T K_T N_L}{(K_T C_L + N_L)^2} \right]. \tag{14}$$

Having the detailed expressions of θ_T in **(12)** and D^* in **(14)**, we finally obtain the following equation:

$$\begin{aligned} &\left(\left[1 + \frac{N_T K_T N_L}{(K_T C_L + N_L)^2} \right] \frac{\partial C_L}{\partial t}, C_L^* \right) + \left(D_L \nabla C_L, \nabla C_L^* \right) \\ &- \left(\frac{C_L D_L \bar{V}_H}{RT} \nabla \sigma_h, \nabla C_L^* \right) + \left(C_L \frac{K_T}{K_T C_L + N_L} \frac{dN_T}{d\varepsilon_p} \frac{\partial \varepsilon_p}{\partial t}, C_L^* \right) = 0, \end{aligned} \tag{15}$$

where $(A, B) = \int_\Omega A \cdot B d\Omega$.

3. Our numerical scheme

For our numerical scheme, we make the choice that all the terms have unknown parts. The motivation of this choice is to avoid some computational difficulties which appear with the increase of $|\nabla \sigma_h|$ in the Krom et al. scheme [2]. By this new scheme, we can solve high Péclet number problems with suitable stabilization techniques. Furthermore, we need an explicit form for $\dfrac{dN_T}{d\varepsilon_p} \dfrac{\partial \varepsilon_p}{\partial t}$. For the number of trap sites N_T, the following expression, also used by Sofronis and McMeeking[1] and Krom et al.[2] before, is used:

$$\log_{10}(N_T) = 23.26 - 2.33\, e^{-5.5\varepsilon_p}. \tag{16}$$

Using this relation, we can have the expression for $\frac{dN_T}{d\varepsilon_p}\frac{\partial \varepsilon_p}{\partial t}$:

$$\begin{cases} \dfrac{\partial \varepsilon_p}{\partial t} \approx \dfrac{\varepsilon_p^{n+1} - \varepsilon_p^n}{\Delta t}, \\ \dfrac{dN_T}{d\varepsilon_p} = N_T * \log_e 10 * (12.815)\, e^{-5.5\varepsilon_p}. \end{cases} \tag{17}$$

After having the expression for $\frac{dN_T}{d\varepsilon_p}\frac{\partial \varepsilon_p}{\partial t}$ with the finite difference in time (Δt : the time step) in **(17)**, we get the following implicit scheme,

$$\begin{aligned} &\left(\left[1 + \frac{N_L K_T N_T(\varepsilon_p^n)}{(K_T C_L^n + N_L)^2}\right]\left(\frac{C_L^{n+1} - C_L^n}{\Delta t}\right), C_L^*\right) + \left(D_L \nabla C_L^{n+1}, \nabla C_L^*\right) \\ &- \left(\frac{C_L^{n+1} D_L \overline{V}_H}{RT} \nabla \sigma_h^n, \nabla C_L^*\right) + \left(C_L^{n+1} \frac{29.508 K_T N_T(\varepsilon_p^n) e^{-5.5\varepsilon_p^n}}{K_T C_L^n + N_L} \frac{\varepsilon_p^{n+1} - \varepsilon_p^n}{\Delta t}, C_L^*\right) = 0. \end{aligned} \tag{18}$$

As we can see, the above scheme is different from the following Krom et al. implicit scheme,

$$\begin{aligned} &\left(\left[1 + \frac{N_L K_T N_T(\varepsilon_p^n)}{(K_T C_L^n + N_L)^2}\right]\left(\frac{C_L^{n+1} - C_L^n}{\Delta t}\right), C_L^*\right) + \left(D_L \nabla C_L^{n+1}, \nabla C_L^*\right) = \\ &\left(\frac{C_L^n D_L \overline{V}_H}{RT} \nabla \sigma_h^n, \nabla C_L^*\right) - \left(C_L^n \frac{29.508 K_T N_T(\varepsilon_p^n) e^{-5.5\varepsilon_p^n}}{K_T C_L^n + N_L} \frac{\varepsilon_p^{n+1} - \varepsilon_p^n}{\Delta t}, C_L^*\right). \end{aligned} \tag{19}$$

It is noted that (18) produces a non-symmetric coefficient matrix for each time step due to the third term in the left hand side, though (19) makes a symmetric coefficient matrix. It is also noted that ε_p^{n+1} in **(18)** and **(19)** is given with ε_p^n because a structural analysis is performed before the diffusion analysis of hydrogen concentration. The hydrostatic stress σ_h^n is also provided by the stress analysis in the same way. Our final remark is that the backward time difference is adopted as the pioneers[1) 2)] because of its excellent stability character in the sense of the maximum norm.

4. Numerical data and results

4.1 A mesh, boundary conditions and material properties

Some other differences between the Krom et al. computation and ours are mentioned. The software used to perform the stress analysis in our case is ADVENTURE_Solid [5] and related modules; we work on a three-dimensional model, so we use finite elements different from those used by Krom et al.:

- Krom et al.: Q1 elements (2D case),
- Our computation: P2 elements (3D case), see **Fig 2** and **Fig 3**.

The plastic strain and hydrostatic stress data are also obtained before the hydrogen diffusion analysis by using the ADVENTURE Solid software.

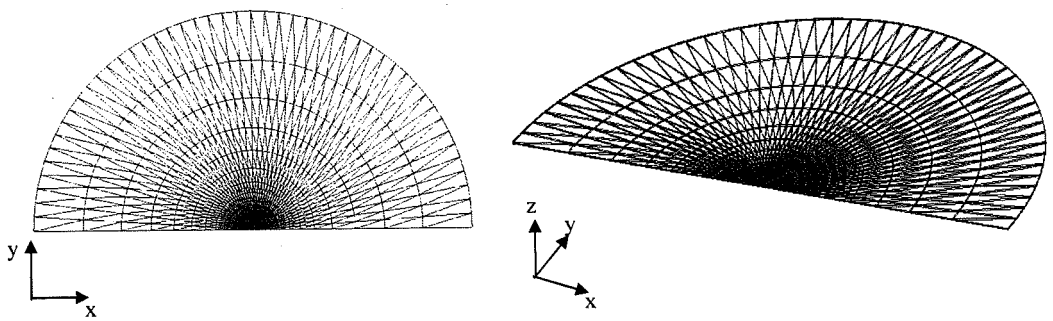

Fig 2. A mesh.

Table 1. Model dimensions.

Crack tip opening b_0	1.0×10^{-5} [m]
Model radius **R**	1.5×10^{-1} [m]
Model thickness h	8.25×10^{-4} [m]

The model is a half circle with a radius of $1.5\times10^{-1}[m]$ and a thickness of $8.25\times10^{-4}[m]$. The crack can be considered as a horizontal band, going from the center to the left until the circumference of the half circle with a thickness of $1.0\times10^{-5}[m]$. A recap of the model dimension is found in **Table 1**.

The mesh consists of 10,656 nodes and 3,706 10-node tetrahedral elements. The mesh is refined near the crack tip.

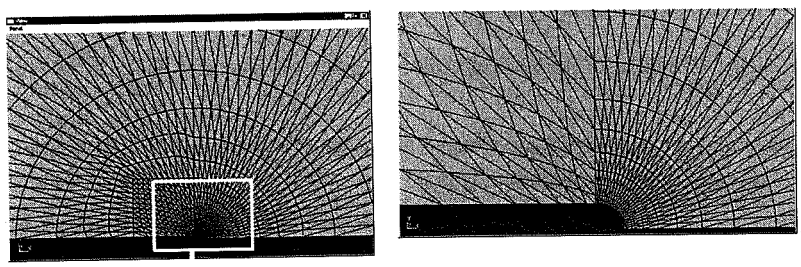

Fig 3. The mesh near the crack tip.

Table 2. Numerical parameters.

Number of elements	3,706
Number of nodes	10,656
CPU	Pentium 4 3.2 GHz
Memory	2.0 GB
CPU time	480~600[s]
Time increment Δt	0.005[s], 0.5 [s], etc...
Total time	1.3[s], 130[s], etc...
Number of total steps	260
Solver	BiCGSTAB(L): L=4
Preconditionner	Shifted ILU (shift value: 1.05)
Convergence criterion for relative residuals in BiCGSTAB (L).	10^{-6}

The BiCGSTAB(L) solver [6] is used with L=4 for the non-symmetric coefficient matrix. The ILU preconditionner is also used with the acceleration parameter which is set to be 1.05. **Table 2** recapitulates the set of numerical parameters used in our computation.

The diffusion analysis and the stress analysis were carried separately. Results produced by the stress analysis such as the hydrostatic stress and the strain rate factor were used to perform the diffusion analysis. Boundary conditions are given as in **Fig 1**. Normally, the boundary condition C_b is given on Γ_E and set to be C_{L0} in this computation. On $\Gamma_N = \partial\Omega - \Gamma_E$ (The symmetry line $\theta = 0$), the hydrogen flux is given as $J \cdot n = 0$. For stress analysis, $u_y = 0$ and $T_x = 0$ on Γ_N, $T = 0$ on the surface of the crack, and the displacement u_i (i=x or y) is given on the other boundary as asymptotic boundary conditions of the singular linear elastic field for the mode I opening ($K_I = 89.2MPa\sqrt{m}$). Here, boundary conditions are explained as for the two dimensional case, but the three dimensional case is straightforward. The diffusion coefficient D_L is $1.27\times10^{-8}[m^2 \cdot s^{-1}]$ and the initial hydrogen concentration C_{L0} is $2.08\times10^{21}[m^{-3}]$ [1) 2)] (4.425×10^{-4} [ppm]). Stress data are provided for 260 steps with a time increment of 0.5[s], which means a total time of 130[s]. The temperature T is fixed at $300[K]$ and the value of the partial molar volume $\overline{V}_H$ is $2.0\times10^{-6}[m^3 \cdot mol^{-1}]$. The number of lattice sites per unit volume N_L is $5.10\times10^{29}[m^{-3}]$ and the trap binding energy ΔE_T is $-60\times10^3[J \cdot mol^{-1}]$. **Table 3** is a recap of the different constant values.

We use the same stress-strain relation as the one used by Krom et al. [2],

$$\varepsilon = \begin{cases} \dfrac{\sigma}{E} & if\ \varepsilon \le \dfrac{\sigma_y}{E} \\ \dfrac{\sigma_y}{E}\left(\dfrac{\sigma}{\sigma_y}\right)^{n'} & if\ \varepsilon > \dfrac{\sigma_y}{E} \end{cases} \tag{20}$$

where E is the Young's modulus: 207[GPa], $\sigma[N \cdot m^{-2}]$ is the applied stress, $\varepsilon[-]$ is the total strain, σ_y=250[MPa] is the yield stress , and n'=5 is the hardening exponent. To be able to use this power law relation, a modification of the ADVENTURE_Solid [5] software has been necessary. This relation is given by Cauchy stresses, but the relation used by Sofronis and McMeeking is different, because it is given by Kirchoff stresses [1) 2)].

Table 3. Constant values.

Diffusion constant	D_L	$1.27\times10^{-8}[m^2 \cdot s^{-1}]$
Gas constant	R	$8.3144[J \cdot mol^{-1} \cdot K^{-1}]$
Temperature	T	$300[K]$
Initial hydrogen concentration	C_{L0}	$2.08\times10^{21}[m^{-3}]$
Partial molar volume of hydrogen	$\overline{V}_H$	$2\times10^{-6}[m^3 \cdot mol^{-1}]$
Lattice sites per unit volume	N_L	$5.10\times10^{29}[m^{-3}]$
Trap binding energy	ΔE_T	$-60\times10^3[J \cdot mol^{-1}]$
Poisson ratio	ν	0.3[-]
Young modulus	E	207[GPa]
Yield stress	σ_y	250[MPa]

4.2 Results

We first consider stress analysis results, comparing our hydrostatic stress (the vertical axis) distribution ahead of the crack tip in the line ($\theta = 0^\circ$) with those of two previous papers [1) 2)] in **Fig 4**. We have on the horizontal axis the ratio on the radial component r over the crack tip opening displacement $b = 4.7b_0$. The crack grows at each step, the stress intensity factor is $K_I = 89.2[MPa\sqrt{m}]$, σ_h is the hydrostatic stress, and σ_y is the yield stress. The results are provided for a loading time of 130[s].

As we can see in **Fig 4**, our results match well with Krom et al. hydrostatic stress. But some differences are observed around the center of the model. This is probably due to the difference in the type of elements, especially around the center where our mesh is refined.

Now we compare the hydrogen distribution in lattice sites at 130[s] with Krom et al. results in **Fig 5**. The results with the strain rate factor and without the strain rate factor are computed for a loading time of 130[s]. C_{L0} is the initial hydrogen concentration, and again $\theta = 0^\circ$. Effects of the strain rate factor can be observed in both results. Good agreement is shown.

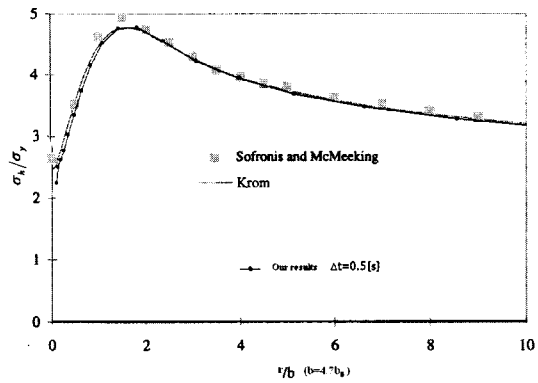

Fig 4. Hydrostatic stress comparison.

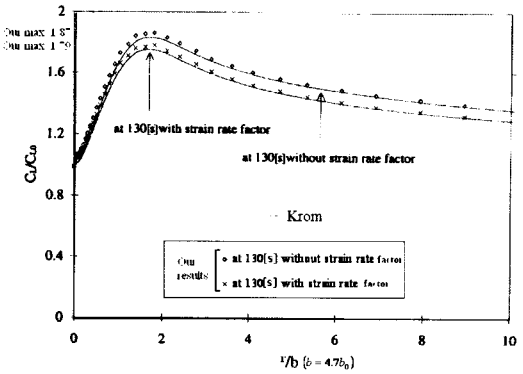

Fig 5. $\left(C_L/C_{L0}\right)$ ahead of the crack tip by our scheme and by Krom et al. scheme at 130[s] (end of loading).

We extend the comparison of hydrogen distribution in lattice sites by computing it for several loading times. We keep $K_I = 89.2[MPa\sqrt{m}]$, and the hydrogen concentration is prescribed on the crack surface.

We notice that the hydrogen concentration obtained with our scheme is the same as the concentration obtained with the Krom et al. scheme for several loading times in **Fig 6**.

In **Fig 7**, we observe the variations of hydrogen concentration in trap sites. In Krom et al. results, hydrogen concentration distribution in trap sites is given for a loading time of 1.3[s], and for loading times going from 3.25[s] to 1.3×10^6[s]. The concentration of hydrogen in trap sites is sensibly the same. As we can see, our results are quite close to Krom et al. results [2]. In our case, we also consider a loading time of 1.3[s], and we consider another loading time included between 3.25[s] and 1.3×10^6[s], i.e. 130[s]. The concentration peak in trap sites is approximately 86 times the initial concentration in lattice sites. According to Krom et al., even though the strain has a slight effect on hydrogen concentration in trap sites for the considered loading times, the trapping of hydrogen is necessary to get a significant impact of the strain rate on hydrogen concentration in lattice sites.

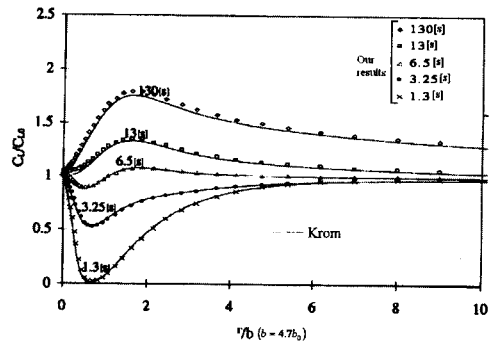

Fig 6. $\left(C_L/C_{L0}\right)$ ahead of the crack tip by our scheme and by Krom et al. scheme for different loading times.

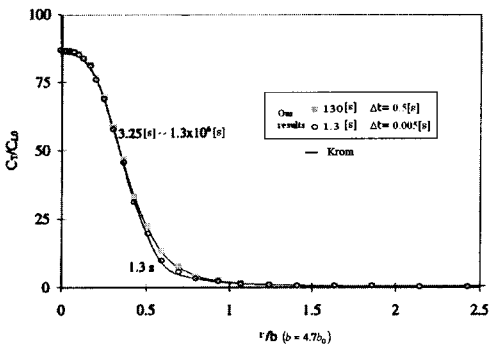

Fig 7. $\left(C_T/C_{L0}\right)$ ahead of the crack tip for different loading times.

5. Conclusion

Using the Sofronis and McMeeking model, we have reconstructed our own finite element scheme based on the Krom et al. scheme, and applied the Galerkin method in this first trial. Results obtained with our new scheme have shown that the scheme can provide good results for this kind problem. Some numerical complications may be encountered for great values of $|\nabla \sigma_h|$. They could be improved by the use of the stabilized method, for example. Fully coupled analysis may also be required; in order to perform a fully coupled analysis, the hydrostatic stress and the strain rate factor should fully depend on the total hydrogen concentration in lattice and trap sites [7) 8)]. Those are our next goals for hydrogen diffusion problems in materials.

Acknowledgment

This research has been conducted as part of "Fundamental Research Project on Advanced Hydrogen Science" funded by New Energy and Industrial Technology Development Organization (NEDO).

References

1) P. Sofronis, R. M. McMeeking, "Numerical analysis of hydrogen transport near a blunting crack tip", *Journal of the Mechanics and Physics of Solids* , Vol. 37 (1989), pp. 317-350.
2) A.H.M. Krom, R.W.J. Koers, A. Bakker, "Hydrogen transport near a blunting crack tip", *Journal of the Mechanics and Physics of Solids* , Vol. 47 (1999), pp. 971-992.
3) R.A. Oriani, "The diffusion and trapping of hydrogen in steel", *Acta Metall.* 18 (1970), pp.147-157.
4) A.Taha, P. Sofronis, "A micromechanics approach to the study of hydrogen transport and embrittlement", Eng. Fracture Mech. 68 (2001), pp.803-837.
5) ADVENTURE PROJECT, http://adventure.q.t.u-tokyo.ac.jp/.
6) G. L. G. Sleijpen, D. R. Fokkema, "BiCGSTAB(L) for linear equations involving unsymmetric matrices with complex spectrum", *ETNA* **1** (1993), pp.11-32.
7) Y. Liang, P. Sofronis, R.H. Dodds Jr., "Interaction of hydrogen with crack tip plasticity: effects of constraint on void growth", *Materials Science and Engineering*, A366 (2004), pp. 397-411.
8) H. Kotake, R. Matsumoto, S. Taketomi, N. Miyazaki, "Unsteady hydrogen diffusion-elastoplastic coupling analysis near a blunting crack tip", Japanese paper submitted to *Transaction of the Japan Society of Mechanical Engineers.*